



โครงการ

การเรียนการสอนเพื่อเสริมประสบการณ์

ชื่อโครงการ การควบคุมระบบควอนตัมแบบเปิดอย่างเหมาะสมโดยใช้ปริพันธ์เชิงวิถี
ของระบบสุ่ม
Optimal Controls for Open Quantum Systems Using
Stochastic Path Integrals

ชื่อนิสิต นายวีระวัฒน์ ก่อแก้ว เลขประจำตัว 6033437823

ภาควิชา ฟิสิกส์

ปีการศึกษา 2563

Optimal Controls for Open Quantum Systems Using Stochastic Path Integrals

Mr. Wirawat Kokaew

A report submitted to the Department of Physics of Chulalongkorn University in
partial fulfillment of the requirements for the degree of
Bachelor of Science in Physics
Academic Year 2020

Project Title Optimal Controls for Open Quantum Systems Using
 Stochastic Path Integrals

By Wirawat Kokaew

Field of Study Physics


Project Advisor Thiparat Chotibut, Ph.D.


Project Co-Advisor Areeya Chantasri, Ph.D.

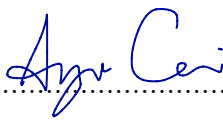
Academic Year 2020

This report is submitted to the Department of Physics, Faculty of Science,
Chulalongkorn University in partial fulfillment of the requirements for the degree of
Bachelor of Science.

This report has been approved by the committee:


..... Chairman
(Assistant Professor Patcha Chatraphorn, Ph.D.)


..... Project Advisor
(Thiparat Chotibut, Ph.D.)


..... Project Co-Advisor
(Areeya Chantasri, Ph.D.)


..... Committee
(Associate Professor Surachate Limkumnerd, Ph.D.)

หัวข้อโครงการ	การควบคุมระบบควอนตัมแบบเปิดอย่างเหมาะสมโดยใช้ปริพันธ์เชิงวิถีของระบบสุ่ม		
ชื่อนิติ	วิระวัฒน์ ก่อแก้ว	รหัสประจำตัวนิติ	6033437823
ภาควิชา	ฟิสิกส์		
อาจารย์ที่ปรึกษา	อ. ดร. ธิปรัชต์ โชติบุตร		
อาจารย์ที่ปรึกษาร่วม	อ. ดร. อารีญา จันทศรี		
ปีการศึกษา	2020		

บทคัดย่อ

การควบคุมระบบควอนตัมแบบเปิดคือการควบคุมการวิวัฒนาการของระบบควอนตัมที่ถูกรบกวนจากสิ่งแวดล้อม วิธีดั้งเดิมสำหรับอธิบายการวิวัฒนาการของระบบควอนตัมแบบเปิดคือการวิวัฒนาการแบบลินบลัด (Lindblad evolution) สามารถอธิบายถึงวิถีเฉลี่ย (Mean path) ของการวิวัฒนาการทั้งหมดที่เป็นไปได้ของระบบควอนตัมแบบเปิด แต่อย่างไรก็ตามในกรณีที่การกระจายตัวของสถานะสุดท้ายของระบบไม่กระจายตัวรอบสถานะที่คาดหวัง ดังนั้นเส้นทางโดยเฉลี่ยของการวิวัฒนาการจึงไม่ใช่วิถีที่ดีที่สุดสำหรับอธิบายการวิวัฒนาการของระบบควอนตัมแบบเปิด ในโครงการนี้เราจึงนำเสนอวิธีใหม่ซึ่งได้จากการทำปริพันธ์เชิงวิถีของระบบสุ่มสำหรับการวิวัฒนาการของระบบควอนตัมแบบเปิด สามารถอธิบายถึงวิถีที่เป็นไปได้มากที่สุด (Most likely path) ของระบบ ขอบเขตของโครงการนี้คือพิจารณาปัญหาการควบคุมการวิวัฒนาการของระบบควอนตัมสองสถานะหรือคิวบิตโดยถูกรบกวนจากสิ่งแวดล้อมที่เกิดขึ้นขณะการเปลี่ยนสถานะจากสถานะเริ่มต้นไปยังสถานะที่คาดหวังผ่านการควบคุมความถี่ราบี (Rabi frequency) การควบคุมระบบควอนตัมแบบเปิดโดยใช้วิถีที่เป็นไปได้มากที่สุดให้ผลเป็นสมการเชิงวิเคราะห์ (Analytical solution) ของความถี่ราบีและเวลาที่ใช้ในการควบคุมทั้งหมดในรูปของตัวแปรสถานะเริ่มต้นและสถานะที่คาดหวังซึ่งไม่สามารถทำได้จากการวิวัฒนาการของลินบลัด จากการเปรียบเทียบผลของการกระจายตัวของสถานะสุดท้ายระหว่างการควบคุมโดยใช้วิถีที่เป็นไปได้มากที่สุดและวิถีการวิวัฒนาการของลินบลัด พบว่าการควบคุมโดยใช้วิถีที่เป็นไปได้มากที่สุดให้ผลสถานะสุดท้ายกระจายตัวรอบสถานะที่คาดหวังซึ่งเหมาะแก่การควบคุมคิวบิตมากกว่าวิถีการวิวัฒนาการของลินบลัด

คำสำคัญ: การควบคุมระบบควอนตัมแบบเปิด, วิถีที่เป็นไปได้มากที่สุด, ปริพันธ์เชิงวิถีของระบบสุ่ม

Project Title	Optimal Controls for Open Quantum Systems Using Stochastic Path Integrals
By	Wirawat Kokaew
Field of Study	Physics
Project Advisor	Thiparat Chotibut, Ph.D.
Project Co-Advisor	Areeya Chantasri, Ph.D.
Academic Year	2020

ABSTRACT

We propose a new optimal control protocol for quantum state preparation in the presence of environmental noises based on the Most Likely Path (MLP) approach. The standard method for dealing with unknown noises in open quantum systems is via Lindblad master equation, which describes the Mean Path (MP) of noisy quantum trajectories. However, the mean path does not always faithfully represent the ensemble of trajectories, especially when the trajectory distribution is multimodal. The most likely path of quantum trajectories is extracted from stochastic path integral formulation, constructed from the joint probability of quantum state trajectories and the noises. We study a quantum control problem of a single-qubit state preparation, controlling the qubit from an arbitrary initial state to the desired target state in the presence of a dephasing noise, where the control is the Rabi oscillation. This approach yields the analytical solution for the optimal control protocol for the Rabi drive, which is not possible using the standard MP approach. We also investigate the benefits of optimal Rabi drive by looking at the distribution of final states in the Bloch sphere; we find that the distribution of final state is concentrated around the desired target state and does not spread out over the qubit.

Keywords: Controlling open quantum systems, Most likely path, Stochastic path integrals

ACKNOWLEDGEMENTS

All the trees have roots. I would like to start by expressing my deepest gratitude to my advisors Dr. Thiparat Chotibut and Dr. Areeya Chantasri, for bringing me into this exciting and rapidly growing field of open quantum systems. They have comprehensive knowledge in both fundamental and applied science. I learned a lot of interesting new ideas through our research interactions and I really enjoyed it.

I wish to thank the committee, Assistant Professor Patcha Chatraphorn and Associate Professor Surachate Limkunnerd, for advice and suggestions. I would like to thank, the lecturers, staff officers, and my colleagues for the four years intensive physics at the department of Physics, Chulalongkorn University.

Last but not least, I want to express my gratefulness to my family, who continuously supports, encourages and accompanies me.

Contents

Abstract	i
Acknowledgements	ii
Contents	iii
List of Figures	v
1 Introduction	1
2 Background on Open Quantum Systems	4
2.1 Open quantum systems	4
2.1.1 Bloch sphere representation	6
2.1.2 Noise and decoherence	7
2.2 Lindblad master equation	8
2.3 Open Quantum System Dynamics and Stochastic Processes	9
2.4 Measures for state preparation controls	11
3 Optimal Control for State Preparation via the Most Likely Path	13
3.1 Stochastic Path Integral for Open Quantum Systems	14
3.1.1 Theoretical Formulation of the Stochastic Path Integral	14
3.1.2 The Most Likely Path for Qubit State Preparation	15

3.1.3	The Most Likely Path for Qubit State Preparation without Rabi Oscillation ($\Delta = 0$)	15
3.1.4	The Most Likely Path for Qubit State Preparation with Rabi Oscillation ($\Delta \neq 0$)	17
3.2	Optimal Rabi Drive for Qubit State Preparation	19
4	Evaluation, Analysis and Comparisons	22
5	Conclusions	30
	Bibliography	32
A	Derivation	35
A.1	Ito Stochastic differential equations to Lindblad master equation	35
A.2	The analytical solution of the most likely path in state preparation without Rabi oscillation ($\Delta = 0$)	36
A.3	Rabi drive and total time duration control	38
B	Distance measure	40
B.1	Trace distance	40
B.2	Fidelity	41

List of Figures

2.1 Bloch sphere representation.	6
2.2 Transverse and longitudinal noise represented on the Bloch sphere.	8
3.1 The most likely paths from solving Eq. (3.16) numerically.	19
4.1 An example where we control qubit state by the optimal Rabi drive and optimal total duration time.	22
4.2 The comparison of quantum trajectories and the fidelity between using arbitrary controls and optimal control form the most likely path in Bloch sphere representation.	23
4.3 The comparison of final state distribution between using arbitrary controls and optimal control from the most likely path in spherical coordinate.	24
4.4 An example where the most likely path's prediction of the Rabi drive does not coincide with the optimal Rabi drive from the mean path. (Minimize trace distance).	25
4.5 The trajectory results (x -component of the qubit) using the optimal Rabi drive from the mean path (numerical search for the minimized trace distance using the Lindblad master equation) and the most likely path (Analytic solution).	26
4.6 An example of the prediction of the optimal Rabi drive from the most likely path does not coincide with the optimal Rabi drive from the mean path. (Maximize fidelity).	27

4.7	The results of distribution of final states in the spherical coordinate, controlled by the optimal Rabi drive from the most likely path and the mean path approaches.	28
4.8	The comparison between the most likely path and the mean path approaches in maximizing the average fidelity to the target state.	29

Chapter 1

Introduction

The theory of open quantum systems is at the core of nearly all modern research in quantum mechanics and its applications [1, 2, 3]. Perfectly unitary quantum dynamics is rarely achievable in experiments, since the experimental system must be isolated perfectly from the environment. In reality, every experimental system is open, meaning that it is coupled to some degree to an environment. One challenge in the field of open quantum systems, where the noisy environment can destroy desirable quantum coherence, is to effectively control and manipulate a quantum system in the presence of uncontrollable environmental noise.

Controlling open quantum systems has become a central task in the development of quantum technologies, and quantum control has witnessed rapid progress in the last two decades [4, 5]. For example, effectively manipulating quantum states of Nitrogen Vacancy (NV) centers in diamonds and of superconducting qubits are important stepping stones for constructing useful quantum computing hardware [6]. The general goal of quantum control is to actively control the dynamics of quantum systems to achieve desired objectives; e.g., high fidelity and fast control. The two main fundamental problems in quantum control include controllability of quantum systems and designing control protocols to achieve expected systems performance.

The traditional method for investigating the dynamics of an open quantum system is

via a Markovian master equation in Lindblad form, which contains both unitary dynamics and non-unitary dynamics as a result of interacting with the environment. Optimal controls are typically obtained from *numerically* searching for optimal parameters that maximize the fidelity between the controlled final state and the target state. This can be done by direct evaluation of the extremum condition or by building in monotonic convergence a priori using Krotov's method (e.g. GRAPE algorithm see [7]).

As opposed to the standard Lindblad approach whose optimal control can only be found via numerical search, this project proposes an alternative way that allows for a more systematic optimization scheme that is also analytically tractable. The approach is based on a stochastic path integral formalism of noisy quantum dynamics, which allows one to find a faithful representative path of noisy trajectories ensemble via the Most Likely Path (MLP), or the path most taken [8]. Such approach is proven useful in analyzing representative dynamics of experimental superconducting qubits [9]. In this project, we will construct the stochastic path integral for open quantum systems, and propose the new control scheme whose optimal control parameters are analytically solvable and depend explicitly on the initial state and the desired target state.

This project is organised as follows. Chapter 2, we introduce the background knowledge necessary to understand the control problems in open quantum systems. We begin with the description of open quantum systems in two approaches: the measurement problem, and stochastic Liouville theory. We review the main tool that describes the evolution of a quantum state (two-level system) and also show how environmental noise affects the system dynamics in the Bloch sphere representation. We then explain the standard Lindblad master equation and its consequences for a two-level system with environmental (dephasing) noise. Moreover, we also review the relationship between open quantum dynamics and stochastic process, deriving the evolution of open quantum system in the Bloch sphere coordinate. At the end of this chapter, we review the controlling of open quantum systems using the traditional method, the Lindblad master equation, and end up

with the distance measure for measuring the success of control in open quantum system.

In Chapter [3](#), The Stochastic Path Integral (SPI) formulation for open quantum dynamics is first discussed.. We then discuss how to adopt SPI for controlling the quantum state from the initial state to the desired target state, referred to as *qubit state preparation*. We then apply SPI to the two open systems examples: (i) qubit state preparation without Rabi oscillation, where we derive the analytic solution of the most likely path and (ii) qubit state preparation with the Rabi oscillation, where we verify the analytical results with numerical simulation showing excellent agreement. SPI allows one to obtain the analytic solution for both the optimal Rabi drive and the total control time. Such a solution corresponds to the most likely path connecting the initial state to the desired target state. We demonstrate the success of this MLP control protocol with its high control state fidelity, and also discuss the advantage of the MLP approach. In Chapter [4](#), we elucidate the advantage of the MLP approach by showing the result of the situation when the MLP and the standard Lindblad mean path give significantly different optimal Rabi drive. Finally, we conclude in Chapter [5](#) with topics for further investigations.

Chapter 2

Background on Open Quantum Systems

Textbook theory of quantum mechanics consists of studying idealized closed quantum systems. A closed quantum system is assumed to be isolated from the rest of the Universe, and can be totally described by its Hamiltonian, \mathcal{H} . In practice, experimental quantum systems cannot be completely isolated; they are open and must be coupled with their environments to some degree. This chapter provides the necessary background of the open quantum systems theory [10, 11], which plays a crucial role in the development of optimal control experimental quantum systems.

2.1 Open quantum systems

The most general approach to model open quantum systems is to consider the “measured system” [12]. The measured system consists of the principal system of interest, denoted by ρ_s , coupled to a second system, commonly referred to as the environment or a measurement device, denoted by ρ_e . We assume, however, that the combined system is a closed system and changes over time t by a unitary transformation \hat{U}_t where $\hat{U}_t = \mathcal{T} \exp\left(-i \int_0^t dt' \hat{H}(t')\right)$, and \mathcal{T} is the usual time-ordering operator. At any point in time, the dynamics of the combined system are given by $\varrho_t = \hat{U}_t(\rho_{s,0} \otimes |e_0\rangle\langle e_0|)\hat{U}_t^\dagger$. Let us denote $|e_k\rangle$ to be an orthonormal basis for state space of the environment, and the initial state is $\rho_e = |e_0\rangle\langle e_0|$. By tracing out the environment’s degree of freedom, the reduced

dynamics of the principal system can be obtained. This leads to a dynamical selection of a distinct set of pure states of the open system and counteracts the superposition principle in the Hilbert space of the open system:

$$\mathrm{Tr}_e(\varrho_t) = \sum_k \langle e_k | \hat{U}_t(\rho_{s,0} \otimes |e_0\rangle\langle e_0|) \hat{U}_t^\dagger | e_k \rangle, \quad (2.1)$$

where Tr_e is a trace over the environment's degree of freedom. It is worth noting that, for most of the system-environment coupling, after tracing out the environment, the purity (see [2.1.1](#)) is always lower than the original state. This effect is called *decoherence*, or a dynamical destruction of quantum coherence [\[13\]](#).

In specific regimes, the effects of environment on the principal system can be described simply as a noisy unitary dynamics on ρ_s . We can then use stochastic Liouville theory for this case. This can also be understood as that the principal quantum system is perturbed by classical noise and has a deterministic and stochastic Hamiltonian at any given time. It has the form in the simplest case.

$$\mathcal{H}_{tot}(t) = \mathcal{H}_{det} + \eta(t)\mathcal{H}_N, \quad (2.2)$$

where \mathcal{H}_{det} is the deterministic Hamiltonian, and the stochastic time dependence described by the noise $\eta(t)$ multiplying the noise generator \mathcal{H}_N , modeling the stochastic interaction with the environment [\[14\]](#). In this work, we consider the simple model of open quantum system setup: a single qubit (a two-level system) that evolves unitarily with the pure dephasing noise that drives the qubit's energy fluctuations. The qubit has the energy gap $\epsilon_0 + \epsilon_1\eta(t)$, where $\eta(t)$ is the Gaussian dephasing noise. The controllable Rabi's frequency (drive) is denoted by Δ along the σ_x . The Hamiltonian of the system is then

$$\mathcal{H} = \frac{1}{2}(\epsilon_0 + \epsilon_1\eta(t))\sigma_z - \frac{1}{2}\Delta\sigma_x. \quad (2.3)$$

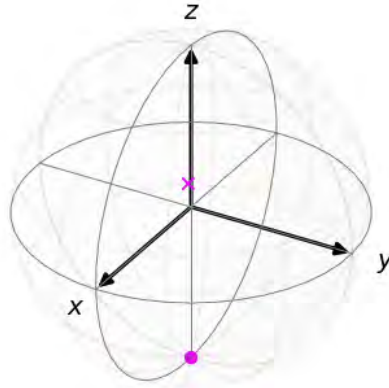


Figure 2.1: Bloch sphere representation. Each component of a Bloch vector q is calculated by expectation of pauli matrix, such as $x = \text{Tr}(\rho\sigma_x)$. The magenta point represents the initial state $\mathbf{q}_I = (0, 0, -1)$, and the magenta cross represents the final state $\mathbf{q}_F = (0.7, 0.39, 0.6)$.

2.1.1 Bloch sphere representation

The Bloch sphere (Bloch ball ^[1]) is a geometrical representation of pure single-qubit states (see Fig. ^[2.1]); i.e., such a pure state can be represented as a point on the unit sphere, and a mixed state can be represented as a point inside the unit sphere. Operations on single qubits can also be represented as Bloch sphere state operations. The orthonormal basis states containing the excited state and ground state correspond to the north and south poles of the Bloch sphere. A point on the unit sphere represents an arbitrary single-qubit state up to the global phase. This Bloch sphere picture is elegant and powerful for the single qubit. It helps in the visualization of quantum state evolution from initial to final states, as well as the investigation of the effects of noise on qubit evolution. For a qubit state, the general form in the Bloch sphere representation is given by the density matrix.

$$\rho \equiv \frac{1}{2}(\mathbb{I} + \mathbf{q} \cdot \boldsymbol{\sigma}) = \frac{1}{2} \begin{pmatrix} 1 + z & x - iy \\ x + iy & 1 - z \end{pmatrix} \quad (2.4)$$

¹Physicists are always messing up the difference between a sphere and ball and mathematicians are always making this discussion.

where $\mathbf{q} = (x, y, z)$ is a Bloch vector and $\boldsymbol{\sigma} = (\sigma_x, \sigma_y, \sigma_z)$ are the Pauli matrices: x, y, z are Bloch sphere components defined by $x = \text{Tr}(\rho\sigma_x)$, $y = \text{Tr}(\rho\sigma_y)$ and $z = \text{Tr}(\rho\sigma_z)$. The size of the Bloch vector can also inform us about the purity of a quantum state which is defined as $\mathcal{P} = \text{Tr}[\rho^2]$. One can show that, for a qubit state, $\mathcal{P} = \frac{1}{2}(1 + \|\mathbf{q}\|^2)$. Therefore, when $\|\mathbf{q}\|^2 = 1$, it is referred to as a pure state, and when $\|\mathbf{q}\|^2 < 1$, it is referred to as a mixed state. To summarise, pure states are represented on the surface of the unit sphere, while mixed states are represented on the interior.

2.1.2 Noise and decoherence

Uncontrollable physical processes in the qubit control, measurement equipment, and the environment surrounding the quantum processor are sources of noise that lead to the decoherence and the reduction of the fidelity of the qubits [15].

In a closed quantum system, the dynamical evolution of a quantum state is deterministic. Meaning that, if we know the initial state and its Hamiltonian, then we can make a prediction of the state of the qubit at any time in the future with certainty. However, the situation changes in the theory of the open quantum system. The quantum system now interacts with uncontrolled degrees of freedom in its environment, which we refer to as noise. We can thus at best aim to predict the probability of finding certain quantum states in the future. We now discuss different roles of noise in our qubit system, i.e., transverse noise and longitudinal noise (see Fig. 2.2).

In Figure 2.2 (a) **T1 Longitudinal relaxation**: the energy exchange between the qubit and its environment, then transverse noise that couples to the qubit in the xy plane and drives transitions from excited state to ground state. The excited state emits energy to the environment and relaxes to ground state at a rate $\Gamma_{1\downarrow}$ (Yellow). Similarly, a qubit in the ground state absorbs energy from the environment, exciting it to an excited state at a rate $\Gamma_{1\uparrow}$ (Blue). In practice, the $\Gamma_{1\uparrow}$ is suppressed, resulting in $\Gamma_1 = \Gamma_{1\downarrow}$ as the total decay rate. It is clear that the appropriate Lindblad operator must effect the transition

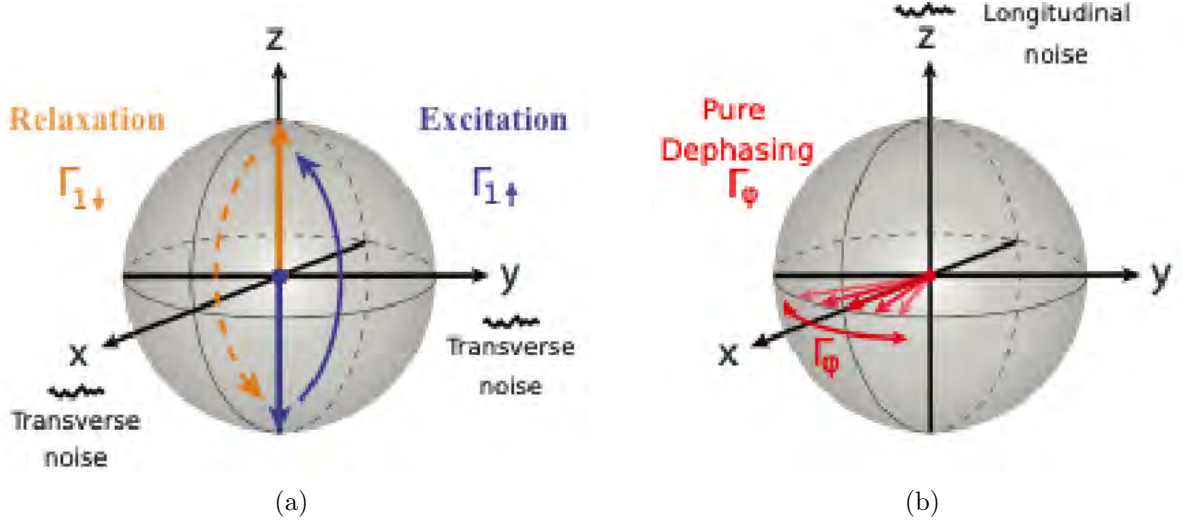


Figure 2.2: Transverse and longitudinal noise represented on the Bloch sphere. (a) Longitudinal relaxation results from energy exchange between the qubit and its environment. (b) Pure dephasing results from fluctuation of qubit energy. See [15] for more details.

$|1\rangle \rightarrow |0\rangle$, this suggests $\hat{L} = \sqrt{\Gamma_1}|0\rangle\langle 1| = \sqrt{\Gamma_1}\sigma_-$.

In Figure 2.2 (b) **Pure dephasing**: the transverse plane arises from longitudinal noise along the z -axis that fluctuates the qubit frequency. Due to stochastic frequency fluctuations, a Bloch vector along the x -axis will diffusely rotate along the z -axis, depolarizing the azimuthal phase with a rate Γ_φ (red). It induces decay of the off-diagonal elements. The appropriate Lindblad operator in this case is $\hat{L} = \sqrt{\Gamma_\varphi/2}\sigma_z$. Decoherence is the leakage of information from a system into the environment, and it occurs at a rate $\Gamma_2 = \Gamma_1/2 + \Gamma_\varphi$ as a result of a combination of energy relaxation and pure dephasing. We also note that in our model the strength of noise ϵ_1 is $\epsilon_1 = 2\sqrt{\Gamma_\varphi/2}$.

2.2 Lindblad master equation

We are interested in dynamics of open quantum system with a strong Markov assumption [16]. The dynamics of open quantum systems Eq. (2.1), after tracing out the interacting environment's degree of freedom, was found to be described by a master equation. In this case, the most general quantum dynamics is generated by the Lindblad equation. It was

shown by Lindblad in 1976.

$$\frac{d\rho}{dt} = -i[\hat{H}, \rho] + \sum_{k=1}^K \mathcal{D}[\hat{L}_k](\rho), \quad (2.5)$$

for \hat{H} Hermitian and $\{\hat{L}_k\}$ arbitrary operators. The superoperator \mathcal{D} is defined by $\mathcal{D}[\hat{L}_k](\rho_t) = \hat{L}_k \rho \hat{L}_k^\dagger - (\hat{L}_k^\dagger \hat{L}_k \rho_t + \rho_t \hat{L}_k^\dagger \hat{L}_k)/2$. This form is known as the Lindblad form, and the operators $\{\hat{L}_k\}$ is called Lindblad operators describing the system-environment couplings. To obtain dynamics of this type, it is generally assumed that the system is weakly coupled to the environment (Born approximation) and the environment is very large, allowing the system to effectively interact with different parts of the environment at different times (Markov approximation). As an example, we consider a two-level atom weakly coupled to an infinite number of electromagnetic field modes and the system control is done via the Rabi oscillation that drives the quantum state. We can derive the Lindblad master equation for the two-level system with the Rabi oscillation in the presence of a dephasing noise strength ϵ_1 . This leads to the unitary dynamics with an effective Hamiltonian, $\mathcal{H} = \epsilon_0 \sigma_z/2 - \Delta \sigma_x/2$, and Lindblad operator $\hat{L} = \epsilon_1 \sigma_z/2$ in the Lindblad form given by,

$$\frac{d\rho}{dt} = -\frac{i}{2}[\epsilon_0 \sigma_z, \rho] + \frac{i}{2}[\Delta \sigma_x, \rho] + \frac{\epsilon_1^2}{4} \mathcal{D}[\sigma_z](\rho). \quad (2.6)$$

We can write this equation in terms of the Bloch sphere coordinates

$$\frac{dx}{dt} = -y\epsilon_0 - \frac{x\epsilon_1^2}{2}, \quad (2.7a)$$

$$\frac{dy}{dt} = (x\epsilon_0 + z\Delta) - \frac{y\epsilon_1^2}{2}, \quad (2.7b)$$

$$\frac{dz}{dt} = -y\Delta. \quad (2.7c)$$

2.3 Open Quantum System Dynamics and Stochastic Processes

The stochastic methods, popular in a variety of fields, ranging from physics to economics and mathematics. In many cases, in the investigation of natural processes, all systems

are open, then stochasticity arises every time one considers the dynamics of a system in the environment. The stochastic process which can be described by stochastic differential equation (SDE) [17, 18].

$$\frac{dx}{dt} = \alpha(x, t) + \beta(x, t)\eta(t). \quad (2.8)$$

where $\alpha(x, t)$ and $\beta(x, t)$ are deterministic function and $\eta(t)$ is the indeterministic function referred to noise or fluctuation in the system. Here, we consider the model Eq. (2.3).

Which can be written as difference equations,

$$x_{k+1} = x_k - y_k \epsilon_0 \delta t - \frac{x_k \epsilon_1^2 \delta t}{2}, \quad (2.9a)$$

$$y_{k+1} = y_k + (x_k \epsilon_0 + z_k \Delta) \delta t - \frac{y_k \epsilon_1^2 \delta t}{2}, \quad (2.9b)$$

$$z_{k+1} = z_k - y_k \Delta \delta t. \quad (2.9c)$$

Adopting the Stratonovich's SDE, which can be obtained by expanding $\rho_{k+1} = e^{-i\hat{H}(t)\delta t} \rho_k e^{i\hat{H}(t)\delta t}$ to first order in $\delta t \rightarrow dt$ and using Stratonovich's prescription, we obtain the Lindblad equation

$$\frac{d\rho}{dt} = \frac{i}{2} [\Delta \hat{\sigma}_x, \rho] - \frac{i}{2} [(\epsilon_0 + \epsilon_1 \eta(t)) \hat{\sigma}_z, \rho]. \quad (2.10)$$

In the Bloch vector coordinate, we obtain the updated state equation $\mathbf{q}_{k+1} = \mathcal{E}[\mathbf{q}_k, \eta_k]$, where $\mathcal{E}[\mathbf{q}_k, \eta_k]$ is defined as a function that determines the qubit state at the next infinitesimal time,

$$x_{k+1} = x_k - (\epsilon_0 y_k + \epsilon_1 \eta_k y_k) \delta t, \quad (2.11a)$$

$$y_{k+1} = y_k + (\epsilon_0 x_k + \epsilon_1 \eta_k x_k + \Delta z_k) \delta t, \quad (2.11b)$$

$$z_{k+1} = z_k - \Delta y_k \delta t. \quad (2.11c)$$

These stochastic differential equations describe the evolution of our qubit in the presence of dephasing noise. The stochastic component η_k arises from interaction with the environment. As a result of different quantum dynamics pathways given by each of the noise realizations, we can collect an ensemble of noisy quantum trajectories.

We also note that, one can interpret this stochastic evolution according to Itô's SDE. By expanding $\rho_{k+1} = e^{-i\hat{H}(t)\delta t}\rho_k e^{i\hat{H}(t)\delta t}$, using the Itô's prescription $\eta^2(t)\delta t^2 \approx \delta t$. Then, averaging over noise realizations and taking the time-continuum limit, $\delta t \rightarrow dt$, we obtain the Lindblad master equation Eq. (2.6) and Eqs. (2.7). This means that the Lindblad master equation produces the *Mean Path* (MP) of quantum trajectories. (see appendix A.1)

2.4 Measures for state preparation controls

State preparation control refers to the ability to accurately steer a dynamical system from an initial to a final state; optimal control does so with the least amount of effort and resources [19].

Quantum control's main objective is to actively manipulate and control the dynamics of quantum systems in order to obtain desired outcomes. The distance between the final state and the target state is one metric for quantum control performance. The projection between the two states can be used as a proxy for fidelity. This is given in terms of the Hilbert Schmidt product of the state of the system at the final state (ρ_F) and the target state (ρ_T):

$$F(\rho_F, \rho_T) = [\text{Tr}(\sqrt{\rho_F^{1/2}\rho_T\rho_F^{1/2}})]^2. \quad (2.12)$$

Another measure is the trace distance, which is widely used in quantum computation and the quantum information community, defined by the equation

$$D(\rho_F, \rho_T) = \frac{1}{2}\text{Tr}|\rho_F - \rho_T|. \quad (2.13)$$

The fidelity and trace distance can be neatly represented in the Bloch sphere representation (see Appendix B for more details). The traditional approach for solving the optimal control problem of an open quantum system is to consider the dynamics of a density matrix ρ represented by a master equation. For the dynamics of a Markovian open quantum system, ρ follows the master equation in the Lindblad form (2.5). Typically, this control

problem is complicated and can not be solved in a closed form. One then needs to resort to numerical optimization; optimization algorithms [20] are obtained by, for instance, seeking an extremum of the fidelity in Eq. (2.12) or the trace distance in Eq. (2.13).

Chapter 3

Optimal Control for State Preparation via the Most Likely Path

We have shown in Chapter [2](#) that one can study the effect of unknown environmental noises in an open quantum systems via Lindblad master equation, which describes a Mean Path (MP) of ensemble quantum trajectories. From a statistics point of view, the mean path may not faithfully represent the ensemble of paths (see Fig. [3.1](#)). We thus needs a new method to control a quantum state from an initial state to the desired target state. One such method investigated in this project is via the Most Likely Path (MLP) method.

Stochastic path integral formalism for continuous quantum measurement [\[8, 21\]](#) is an excellent approach that allows one to represent more faithfully these quantum trajectories via the most likely path a system takes between the two states [\[9\]](#). In this chapter, we adapt the stochastic path integral approach for optimal control of open quantum systems. We can compute the most likely path of the quantum state from an initial state to the desired target state by constructing the stochastic path integral of SDEs.

3.1 Stochastic Path Integral for Open Quantum Systems

3.1.1 Theoretical Formulation of the Stochastic Path Integral

We now construct the probability distribution of quantum trajectories in an open quantum system. A quantum state trajectory is the dynamic of a quantum state. Let us discretize the noise into n time steps and denote $\{\eta_k\}_{k=0}^{n-1}$ as a noise realization. Each η_k is obtained between time t_k and $t_{k+1} = t_k + \delta t$, and is assumed to depend only on a quantum state right before (Markov assumption). We denote a time series of quantum states as $\{\mathbf{q}_k\}_{k=0}^n$. For a two-level quantum system (qubit), $\mathbf{q} = (x, y, z)$ is a vector in Bloch sphere coordinates. The quantum state trajectory can be computed with an updated state equations, as in SDEs Eq. (2.11).

From the SDEs, write the joint probability density function (PDF) of time-discretized state trajectories given an initial state \mathbf{q}_0 and a set of other constraints $\boldsymbol{\alpha}$ as

$$P(\{\mathbf{q}_k\}_{k=1}^n, \{\eta_k\}_0^{n-1} | \mathbf{q}_0, \boldsymbol{\alpha}) = \mathcal{B}_\alpha \prod_{k=0}^{n-1} P(\mathbf{q}_{k+1} | \mathbf{q}_k, \eta_k) P(\eta_k). \quad (3.1)$$

The function \mathcal{B}_α accounts for constraints on the initial and final states. Eq. (3.1) is the product of the deterministic conditional probability distribution and the probability distribution of Gaussian white noise at every time step. The deterministic conditional probability distribution after evolving under Gaussian white noise $P(\mathbf{q}_{k+1} | \mathbf{q}_k, \eta_k) \equiv \delta^d(\mathbf{q}_{k+1} - \boldsymbol{\mathcal{E}}[\mathbf{q}_k, \eta_k])$, $\boldsymbol{\mathcal{E}}[\mathbf{q}_k, \eta_k]$ is the right side of Eqs. (2.11). The probability distribution of Gaussian white noise with zero mean and variance δt^{-1} is $P(\eta_k) = \sqrt{\delta t / (2\pi)} \exp(-\frac{\eta_k^2 \delta t}{2})$.

The path integral representation of the joint PDF in Eq. (3.1) can be attained by writing the delta functions for the updated state equation in Fourier integral form, i.e., $\delta(q) = 1/(2\pi i) \int \exp(-pq) dp$ integrating along contours with end-points at $\pm\infty$ where p is referred to as conjugate variable. Also, by rewriting the $P(\eta_k)$ in exponential form; i.e., $\exp[\ln P(\eta_k)]$.

As a result, the PDF with a fixed initial state $\mathbf{q}_0 = \mathbf{q}_I$ and final state $\mathbf{q}_n = \mathbf{q}_F$ leads to the constraint $\mathcal{B}_\alpha = \delta^d(\mathbf{q}_0 - \mathbf{q}_I)\delta^d(\mathbf{q}_n - \mathbf{q}_F)$ in Eq. (3.1). Then, $\mathcal{P}_{\mathbf{q}_I, \mathbf{q}_F} \equiv P(\{\mathbf{q}_k\}_{k=1}^n, \{\eta_k\}_0^{n-1}, \mathbf{q}_F | \mathbf{q}_I)$ in the path integral form is

$$\mathcal{P}_{\mathbf{q}_I, \mathbf{q}_F} = \mathcal{N} \int \cdots \int \left(\prod_{j=-1}^n d^d p_j \right) \exp(-\mathbf{p}_{-1} \cdot (\mathbf{q}_0 - \mathbf{q}_I) - \mathbf{p}_n \cdot (\mathbf{q}_n - \mathbf{q}_F) + \sum_{k=0}^{n-1} [-\mathbf{p}_k \cdot (\mathbf{q}_{k+1} - \mathcal{E}[\mathbf{q}_k, \eta_k]) - \frac{\eta_k^2 \delta t}{2}]), \quad (3.2)$$

where the constants are absorbed in \mathcal{N} . Thus, the integrals can be written concisely in the form.

$$\mathcal{P}_{\mathbf{q}_I, \mathbf{q}_F} = \mathcal{N} \int d\{\mathbf{p}_k\}_{-1}^n \exp(\mathcal{S}), \quad (3.3)$$

with the action

$$\mathcal{S} = -\mathbf{p}_{-1} \cdot (\mathbf{q}_0 - \mathbf{q}_I) - \mathbf{p}_n \cdot (\mathbf{q}_n - \mathbf{q}_F) + \sum_{k=0}^{n-1} [-\mathbf{p}_k \cdot (\mathbf{q}_{k+1} - \mathcal{E}[\mathbf{q}_k, \eta_k]) - \frac{\eta_k^2 \delta t}{2}] \quad (3.4)$$

3.1.2 The Most Likely Path for Qubit State Preparation

We can extract the most likely path from the ensemble of quantum trajectories specified by Eq. (3.2) by solving for its action's extrema. Taking the variation of the action over all the variables and setting it to zero, we obtain a set of differential equations, extremizing this action over all variables ($k = 0, \dots, n-1$).

$$\frac{\partial \mathcal{S}}{\partial \mathbf{p}_k} = 0, \quad \frac{\partial \mathcal{S}}{\partial \mathbf{q}_k} = 0, \quad \text{and} \quad \frac{\partial \mathcal{S}}{\partial \eta_k} = 0. \quad (3.5)$$

3.1.3 The Most Likely Path for Qubit State Preparation without Rabi Oscillation ($\Delta = 0$)

Pure dephasing arises from longitudinal noise that couples to the qubit via the z-axis. Such longitudinal noise causes the qubit energy ϵ_0 (qubit frequency) to fluctuate without the external Rabi drive. In this case, the Hamiltonian becomes

$$\mathcal{H} = (\epsilon_0 + \epsilon_1 \eta(t)) \frac{\sigma_z}{2}. \quad (3.6)$$

By following section [2.3](#), we can obtain a set of SDEs for time-discretized state evolution. To get updated state equations, expand $\rho_{t+\delta t} = e^{-i\hat{H}(t)\delta t}\rho_t e^{i\hat{H}(t)\delta t}$ to first order in δt and express it in Bloch sphere coordinates:

$$x_{k+1} = x_k - (\epsilon_0 + \epsilon_1\eta_k)y_k\delta t, \quad (3.7a)$$

$$y_{k+1} = y_k + (\epsilon_0 + \epsilon_1\eta_k)x_k\delta t. \quad (3.7b)$$

These equations of motion in two dimensions rotate the state around z -axis of Bloch sphere coordinate with frequency $(\epsilon_0 + \epsilon_1\eta)$. Substitute the updated state equations into the action of qubit state preparation Eq. [\(3.4\)](#). The explicit form of action for the qubit state preparation without Rabi oscillation ($\Delta = 0$) yields

$$\begin{aligned} \mathcal{S} = & -p_{-1}^x(x_0 - x_I) - p_n^x(x_n - x_F) - p_{-1}^y(y_0 - y_I) - p_n^y(y_n - y_F) \\ & - p_{-1}^z(z_0 - z_I) - p_n^z(z_n - z_F) + \sum_{k=0}^{n-1} \left\{ -p_k^x(x_{k+1} - x_k + (\epsilon_0 + \epsilon_1\eta_k)y_k\delta t) \right. \\ & \left. - p_k^y(y_{k+1} - y_k - (\epsilon_0 + \epsilon_1\eta_k)x_k\delta t) - \frac{\eta_k^2\delta t}{2} \right\}. \end{aligned} \quad (3.8)$$

Extremizing this action over all variables ($k = 0, \dots, n - 1$)

$$\frac{\partial \mathcal{S}}{\partial \mathbf{p}_k} = 0, \quad \frac{\partial \mathcal{S}}{\partial \mathbf{q}_k} = 0, \quad \frac{\partial \mathcal{S}}{\partial \eta_k} = 0 \quad (3.9)$$

The following 4 difference equations and 1 constraint,

$$x_{k+1} = x_k - (\epsilon_0 + \epsilon_1\eta_k)y_k\delta t, \quad (3.10a)$$

$$y_{k+1} = y_k + (\epsilon_0 + \epsilon_1\eta_k)x_k\delta t, \quad (3.10b)$$

$$p_k^x = p_{k-1}^x - (\epsilon_0 + \epsilon_1\eta_k)p_k^y\delta t, \quad (3.10c)$$

$$p_k^y = p_{k-1}^y + (\epsilon_0 + \epsilon_1\eta_k)p_k^x\delta t, \quad (3.10d)$$

$$\eta_k = -p_k^x y_k \epsilon_1 + p_k^y x_k \epsilon_1. \quad (3.10e)$$

In time-continuum limit, we obtain the set of the ordinary differential equation and constraint describing the most likely path for qubit with pure dephasing as

$$\dot{x} = -\epsilon_0 y - \epsilon_1 \eta y, \quad (3.11a)$$

$$\dot{y} = +\epsilon_0 x + \epsilon_1 \eta x, \quad (3.11b)$$

$$\dot{p}^x = -\epsilon_0 p^y - \epsilon_1 \eta p^y, \quad (3.11c)$$

$$\dot{p}^y = +\epsilon_0 p^x + \epsilon_1 \eta p^x, \quad (3.11d)$$

$$\eta = -\epsilon_1 p^x y + \epsilon_1 p^y x. \quad (3.11e)$$

Here, we consider the most likely path for qubit state preparation, which can be computed from the ODEs in Eqs. (3.11). We can solve the ODEs analytically (see Appendix A.2 for more details). By explicit calculation, Eqs. (3.11) indicate that $\dot{\eta}$ vanishes. In this case, we conclude that its solution η is constant, and denote $\eta(t) = \eta^*$. The most likely path from Eqs. (3.11) can then be solved. From boundary conditions $\mathbf{q}_I(t=0) = (x_I, y_I)$ and $\mathbf{q}_F(t=T) = (x_F, y_F)$, we obtain

$$x(t) = -y_I \sin(\epsilon_0 t + \epsilon_1 \eta^* t) + x_I \cos(\epsilon_0 t + \epsilon_1 \eta^* t), \quad (3.12a)$$

$$y(t) = +y_I \cos(\epsilon_0 t + \epsilon_1 \eta^* t) + x_I \sin(\epsilon_0 t + \epsilon_1 \eta^* t), \quad (3.12b)$$

$$\eta^* = \left[\arccos \left(\frac{x_I x_F + y_I y_F}{x_I^2 + y_I^2} \right) - \epsilon_0 T \right] / \epsilon_1 T. \quad (3.12c)$$

3.1.4 The Most Likely Path for Qubit State Preparation with Rabi Oscillation ($\Delta \neq 0$)

Here, we extend the analysis to the qubit with an external Rabi drive in x -axis, whereas pure dephasing is caused by longitudinal noise that couples to the qubit via the z -axis. The qubit unitary evolution is described by the Hamiltonian Eq. (2.3)

Expanding $\rho_{t+\delta t} = e^{-i\hat{H}(t)\delta t} \rho_t e^{i\hat{H}(t)\delta t}$ to first order in δt , and expressing it in Bloch

sphere coordinates, we get the updated state equations:

$$x_{k+1} = x_k - (\epsilon_0 y_k + \epsilon_1 \eta_k y_k) \delta t, \quad (3.13a)$$

$$y_{k+1} = y_k + (\epsilon_0 x_k + \epsilon_1 \eta_k x_k + \Delta z_k) \delta t, \quad (3.13b)$$

$$z_{k+1} = z_k - \Delta y_k \delta t. \quad (3.13c)$$

These equations of motion in three dimensions, rotate a state around z-axis of Bloch sphere coordinate with frequency $\epsilon_0 + \epsilon_1 \eta$, and rotate around x-axis with frequency Δ . Substitute the updated state equations into the action of qubit state preparation Eq. (3.4). The explicit form of action for the qubit state preparation with Rabi drive ($\Delta \neq 0$) is

$$\begin{aligned} \mathcal{S} = & -p_{-1}^x(x_0 - x_I) - p_n^x(x_n - x_F) - p_{-1}^y(y_0 - y_I) - p_n^y(y_n - y_F) - p_{-1}^z(z_0 - z_I) \\ & - p_n^z(z_n - z_F) + \sum_{k=0}^{n-1} \left\{ -p_k^x(x_{k+1} - x_k + (\epsilon_0 y_k + \epsilon_1 \eta_k y_k) \delta t) - p_k^y(y_{k+1} \right. \\ & \left. - y_k - (\epsilon_0 x_k + \epsilon_1 \eta_k x_k + \Delta z_k) \delta t) - p_k^z(z_{k+1} - z_k + \Delta y_k \delta t) - \frac{\eta_k^2 \delta t}{2} \right\}. \end{aligned} \quad (3.14)$$

Extremizing this action over all variables ($k = 0, \dots, n - 1$)

$$\frac{\partial \mathcal{S}}{\partial \mathbf{p}_k} = 0, \quad \frac{\partial \mathcal{S}}{\partial \mathbf{q}_k} = 0, \quad \frac{\partial \mathcal{S}}{\partial \eta_k} = 0 \quad (3.15)$$

and taking the time-continuum limit, we obtain the set of the ordinary differential equation and constraint for the most likely path,

$$\dot{x} = -\epsilon_0 y - \epsilon_1 \eta y, \quad (3.16a)$$

$$\dot{y} = +\epsilon_0 x + \epsilon_1 \eta x + \Delta z, \quad (3.16b)$$

$$\dot{z} = -\Delta y, \quad (3.16c)$$

$$\dot{p}^x = -\epsilon_0 p^y - \epsilon_1 \eta p^y, \quad (3.16d)$$

$$\dot{p}^y = +\epsilon_0 p^x + \epsilon_1 \eta p^x, \quad (3.16e)$$

$$\dot{p}^z = -\Delta p^y - \Delta p^z, \quad (3.16f)$$

$$\eta = -\epsilon_1 p^x y + \epsilon_1 p^y x. \quad (3.16g)$$

The most likely path of qubit state preparation with Rabi drive can be solved numerically (see Fig. (3.1)). To verify the most likely path, we numerically simulate qubit state trajectories using odeint (Scipy, Python library). Starting with an initial state $\mathbf{q}_I = (x_I, y_I, z_I)$, a random outcome η_0 is drawn from a distribution of Gaussian white noise, and the next state \mathbf{q}_1 is computed from the update state equation Eq. (3.13). Repeating this computation from $t_0 = 0$ to $t_n = T$ with time step δt produces a single stochastic trajectory for \mathbf{q} .

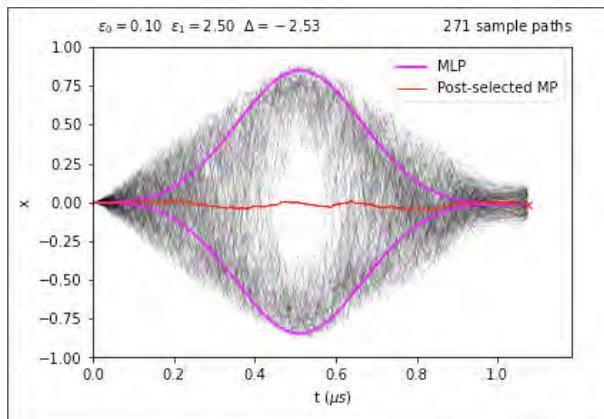


Figure 3.1: The most likely paths (Magenta lines) from solving Eq. (3.16) numerically, the simulated quantum trajectories (Gray lines), the post-selected mean path (Red line). Here, we set the qubit energy $\epsilon_0 = 0.1$, the strength of the dephasing noise $\epsilon_1 = 2.5$, the initial state $\mathbf{q}_I = (0, 0, -1)$, the desired target state $\mathbf{q}_F = (0.01, 0.1, -0.9)$, $\delta t = 0.01$, and the total time duration $T = 1.2$.

3.2 Optimal Rabi Drive for Qubit State Preparation

The ability to extract the most likely path from noisy quantum trajectories offers a new approach to controlling open quantum systems. In this work, we propose an optimal-control scheme for qubit preparation based on the most-likely path (MLP) approach [8]. Using the MLP approach, which concerns the representative path most likely to occur, we study a quantum control problem of a single-qubit state preparation in the presence of a dephasing noise, where the control is the Rabi drive.

By extremizing the action of qubit state preparation in Eq. (3.5) reproduces the Lagrange multiplier method, an optimization strategy that accommodates constraints. Therefore, the optimized function is the last term of action Eq. (3.4) that is $\sum_{k=0}^{n-1} [-\frac{\eta_k^2 \delta t}{2}]$ where the other terms are constraints. The most likely path is a path that optimizes the log-likelihood of quantum trajectory. The Rabi drive is the ability to control the laser pulse that induces the Rabi oscillation in an experiment. Now, let us constrain the Rabi drive at all time steps in order to find the Rabi drive that produces the Most Likely Path. The updated state equations are,

$$x_{k+1} = x_k - (\epsilon_0 y_k + \epsilon_1 \eta_k y_k) \delta_k t, \quad (3.17a)$$

$$y_{k+1} = y_k + (\epsilon_0 x_k + \epsilon_1 \eta_k x_k + \Delta_k z_k) \delta_k t, \quad (3.17b)$$

$$z_{k+1} = z_k - \Delta_k y_k \delta t. \quad (3.17c)$$

Now, the situation changes. The Rabi oscillation (Δ) plays significant role as the parameter in the action,

$$\begin{aligned} \mathcal{S} = & -p_{-1}^x(x_0 - x_I) - p_n^x(x_n - x_F) - p_{-1}^y(y_0 - y_I) - p_n^y(y_n - y_F) - p_{-1}^z(z_0 - z_I) \\ & - p_n^z(z_n - z_F) + \sum_{k=0}^{n-1} \left\{ -p_k^x(x_{k+1} - x_k + (\epsilon_0 y_k + \epsilon_1 \eta_k y_k) \delta t) - p_k^y(y_{k+1} \right. \\ & \left. - y_k - (\epsilon_0 x_k + \epsilon_1 \eta_k x_k + \Delta_k z_k) \delta t) - p_k^z(z_{k+1} - z_k + \Delta_k y_k \delta t) - \frac{\eta_k^2 \delta t}{2} \right\}. \end{aligned} \quad (3.18)$$

Extremizing this action over all variables at all time steps ($k = 0, \dots, n - 1$),

$$\frac{\partial \mathcal{S}}{\partial \mathbf{p}_k} = 0, \quad \frac{\partial \mathcal{S}}{\partial \mathbf{q}_k} = 0, \quad \frac{\partial \mathcal{S}}{\partial \eta_k} = 0, \quad \text{and} \quad \frac{\partial \mathcal{S}}{\partial \Delta_k} = 0 \quad (3.19)$$

In the time-continuum limit, we obtain the 6 ordinary differential equations and 2 con-

straints for describing the most likely path,

$$\dot{x} = -\epsilon_0 y - \epsilon_1 \eta y, \quad (3.20a)$$

$$\dot{y} = +\epsilon_0 x + \epsilon_1 \eta x + \Delta z, \quad (3.20b)$$

$$\dot{z} = -\Delta y, \quad (3.20c)$$

$$\dot{p}^x = -\epsilon_0 p^y - \epsilon_1 \eta p^y, \quad (3.20d)$$

$$\dot{p}^y = +\epsilon_0 p^x + \epsilon_1 \eta p^x + \Delta p^z, \quad (3.20e)$$

$$\dot{p}^z = -\Delta p^y, \quad (3.20f)$$

$$\dot{\eta} = -\epsilon_1 p^x y + \epsilon_1 p^y x, \quad (3.20g)$$

$$p^y z = p^z y. \quad (3.20h)$$

Consider the second derivative of Eq. (3.20h). Such consideration results in the canonical relation between conjugated variables and components of the Bloch sphere vector, i.e, $p^y z = p^z y$, $p^x z = p^z x$ and $p^x y = p^y x$. It means the optimal Rabi drive for qubit state preparation is the path with zero noise realization, $\eta = 0$. This reduces the number of 6 ODEs and 2 constraints to only 3 ODEs. The Rabi drive and the total time duration in analytical forms in terms of the initial state \mathbf{q}_I and desired target state \mathbf{q}_F (see appendix A.3 for more details).

Optimal rabi drive

$$\Delta_{\text{op}}^{\text{MLP}} = \text{sgn}[x_F y_F] \left(\frac{z_I - z_F}{x_F} \right) \epsilon_0, \quad (3.21a)$$

Optimal total time duration

$$T_{\text{op}}^{\text{MLP}} = \arccos \left[1 - \frac{x_F^2 (1 + (\Delta/\epsilon_0)^2)}{(z_I^2 - z_I z_F)} \right] / \sqrt{\Delta^2 + \epsilon_0^2}. \quad (3.21b)$$

Chapter 4

Evaluation, Analysis and Comparisons

In this chapter, we will analyse the performance of the optimal control from the MLP approach in Eq. (3.21a) and (3.21b). We also compare the distribution of the final states with arbitrary controls and optimal controls from the MP approach. The success of control from MLP approach is shown in Fig. (4.1). In Fig. (4.1a), the optimal Rabi drive and

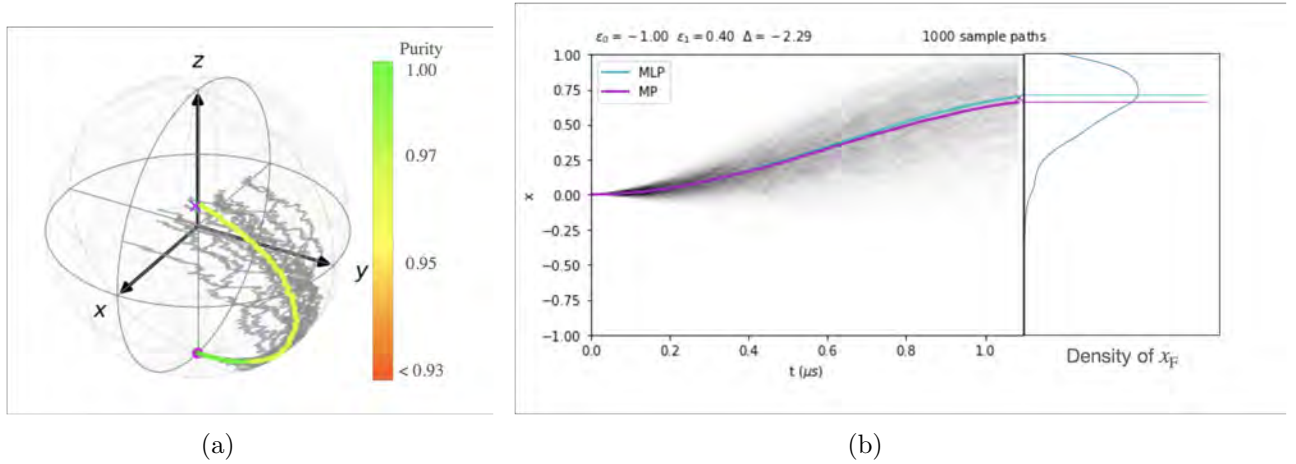


Figure 4.1: An example where we control qubit state by the optimal Rabi drive $\Delta_{\text{op}}^{\text{MLP}} = -2.29$ and optimal total duration time $T_{\text{op}}^{\text{MLP}} = 1.08$. (a) Bloch sphere representation of the desired target state (Magenta cross), the initial state (Magenta point), the quantum trajectories (Gray lines), and the average path (Multi colored line) which color determines the purity of quantum state, (b) the quantum trajectories (Gray lines) in x component of Bloch sphere with the distribution of final states, the mean path (Magenta line), and the most likely path (Cyan line). Here, we set the qubit energy $\epsilon_0 = -1$, the strength of the dephasing noise $\epsilon_1 = 0.40$ initial state $\mathbf{q}_I = (0, 0, -1)$, and the desired target state $\mathbf{q}_F = (0.7, 0.39, 0.6)$. We obtain the high average fidelity $\mathcal{F} \approx 0.97$.

the optimal total time duration yield the high fidelity ($\mathcal{F} \sim 0.97$) connecting the initial state to the desired target state, and the final state distribution concentrates around the desired target state in Fig. (4.1b). We also note that the time scale for controlling qubit state preparation around microseconds ($T \sim \mu s$). In Fig. (4.2), we show that the success of control qubit state with high fidelity by using the optimal Rabi drive and optimal total time duration. The gray line represents noisy quantum state trajectories, while the average path (Multi colored line) represents the purity of the quantum state. The figure shows that the optimal Rabi drive and optimal total time duration produce higher final state purity ($P \sim 0.95$) and fidelity ($\mathcal{F} \sim 0.96$) than arbitrary controls, i.e., the final state purity ($P < 0.93$) and the fidelity ($\mathcal{F} < 0.96$).

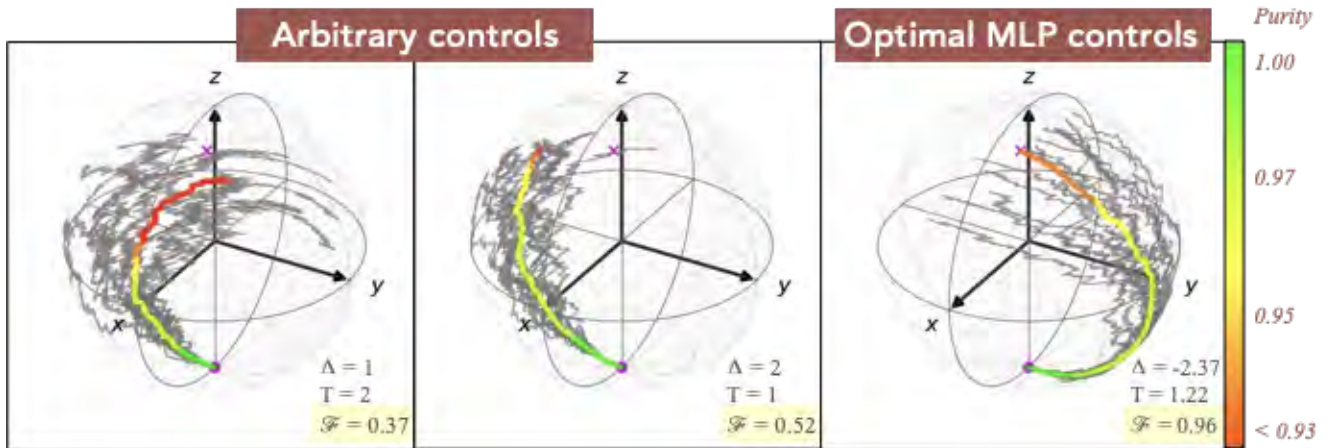


Figure 4.2: The comparison of quantum trajectories and the fidelity between using arbitrary controls and optimal control from the most likely path in Bloch sphere representation of the desired target state (Magenta cross), the initial state (Magenta point), the quantum trajectories (Gray lines) and the average path (Multi colored line) which colour determines the purity of quantum state. In the figure on the left, we set the arbitrary control Rabi drive $\Delta = 1$, the total time duration $T = 2$, then we obtain the bad fidelity $\mathcal{F} = 0.37$. In the figure on the center, we set the arbitrary control Rabi drive $\Delta = 2$, the total time duration $T = 1$, then we obtain the bad fidelity $\mathcal{F} = 0.52$. In the figure on the right, we set the optimal control Rabi drive from the most likely path $\Delta = -2.37$, the total time duration $T = 1.22$, then we obtain the good fidelity $\mathcal{F} = 0.96$. Here, we set the qubit energy $\epsilon_0 = -0.5$, the strength of the dephasing noise $\epsilon_1 = 0.5$, the initial state $\mathbf{q}_I = (0, 0, -1)$, and the desired target state $\mathbf{q}_F = (0.4, 0.17, 0.9)$.

Using the arbitrary control and optimal MLP control in spherical coordinate as shown in Fig. (4.3), we compare the distribution of the final state around the desired target state. We also show that the optimal Rabi drive and total time duration from the most likely path result in a final state distribution that is concentrated on the desired target state. This feature is to be contrasted with the spread out of final quantum states generated from an arbitrary control.

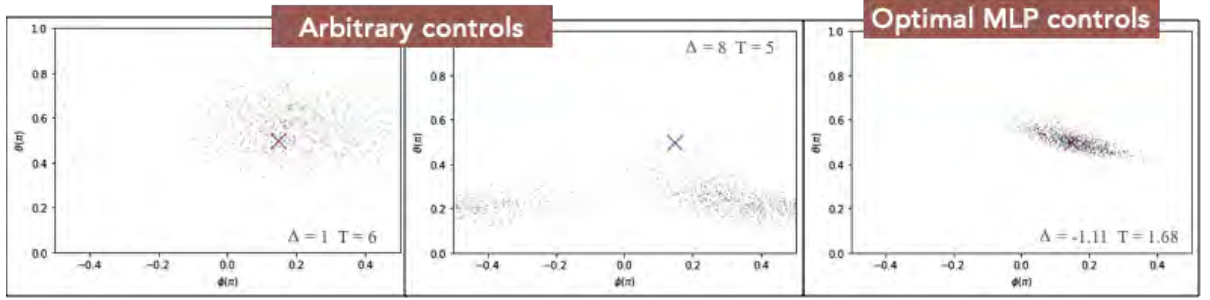


Figure 4.3: The comparison of final state distribution between using arbitrary controls and optimal control from the most likely path in spherical coordinate, the desired target state (Magenta cross), each final state (Black points). In the figure on the left, we set the arbitrary control Rabi drive $\Delta = 1$, the total duration time $T = 6$, then we obtain the spread out of final states and do not concentrate around the target state. In the figure on the center, we set the arbitrary control Rabi drive $\Delta = 8$, the total time duration $T = 5$, then we obtain the spread out of final states and away from the target state. In the figure on the right, we set the optimal control Rabi drive from the most likely path $\Delta = -1.11$, the total time duration $T = 1.68$, then we obtain the final states concentrate around the target state. Here, we set the qubit energy $\epsilon_0 = -1$, the strength of the dephasing noise $\epsilon_1 = 0.3$, the initial state $(\phi, \theta)_I = (0, \pi)$, and the desired target state $(\phi, \theta)_F = (0.14\pi, 0.5\pi)$.

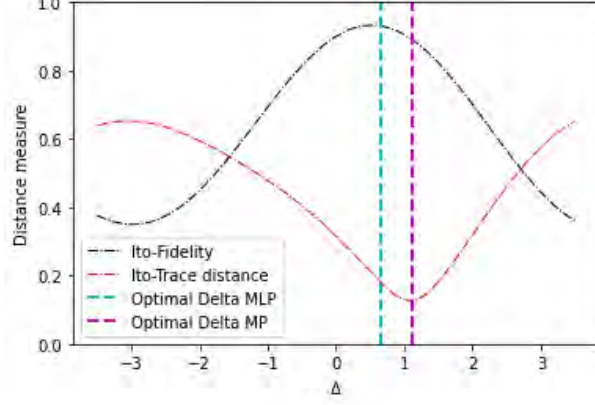


Figure 4.4: An example of the prediction of the Rabi drive from the most likely path, i.e., $\Delta_{\text{op}}^{\text{MLP}} = 0.67$ (Cyan), that does not coincide with the optimal Rabi drive from the mean path $\Delta_{\text{op}}^{\text{MP}} = 1.1$ (Magenta). We use a numerical search with the Lindblad master equation Eq. (2.7) to find the optimal Rabi drive from the mean path by minimizing the trace distance (Red). Here, we set the qubit energy $\epsilon_0 = 1$, the strength of the dephasing noise $\epsilon_1 = 2$, the initial state $\mathbf{q}_I = (0, 0, -1)$, and the desired target state $\mathbf{q}_F = (0.3, -0.52, -0.8)$.

Since the final state distribution as seen in Fig. (4.5 b) does not concentrate around the target state, it is possible that the most likely path approach is a better method to represent the ensemble of quantum trajectories than the traditional mean path (Lindblad) approach. In Fig. (4.4), we use the Lindblad master equation Eq. (2.7) to find the Rabi drive that minimizes the trace distance Eq. (2.13). We obtain a distribution of final states that do not cluster around the target state, as seen in Fig. (4.5 a) and Fig. (4.5 b), generated with the optimal Rabi drive from the mean path approach. However, as shown in Fig. (4.5 c) and Fig. (4.5 d), the Rabi drive from the most likely path approach leads to the distribution of the final states that better concentrates around the target state.

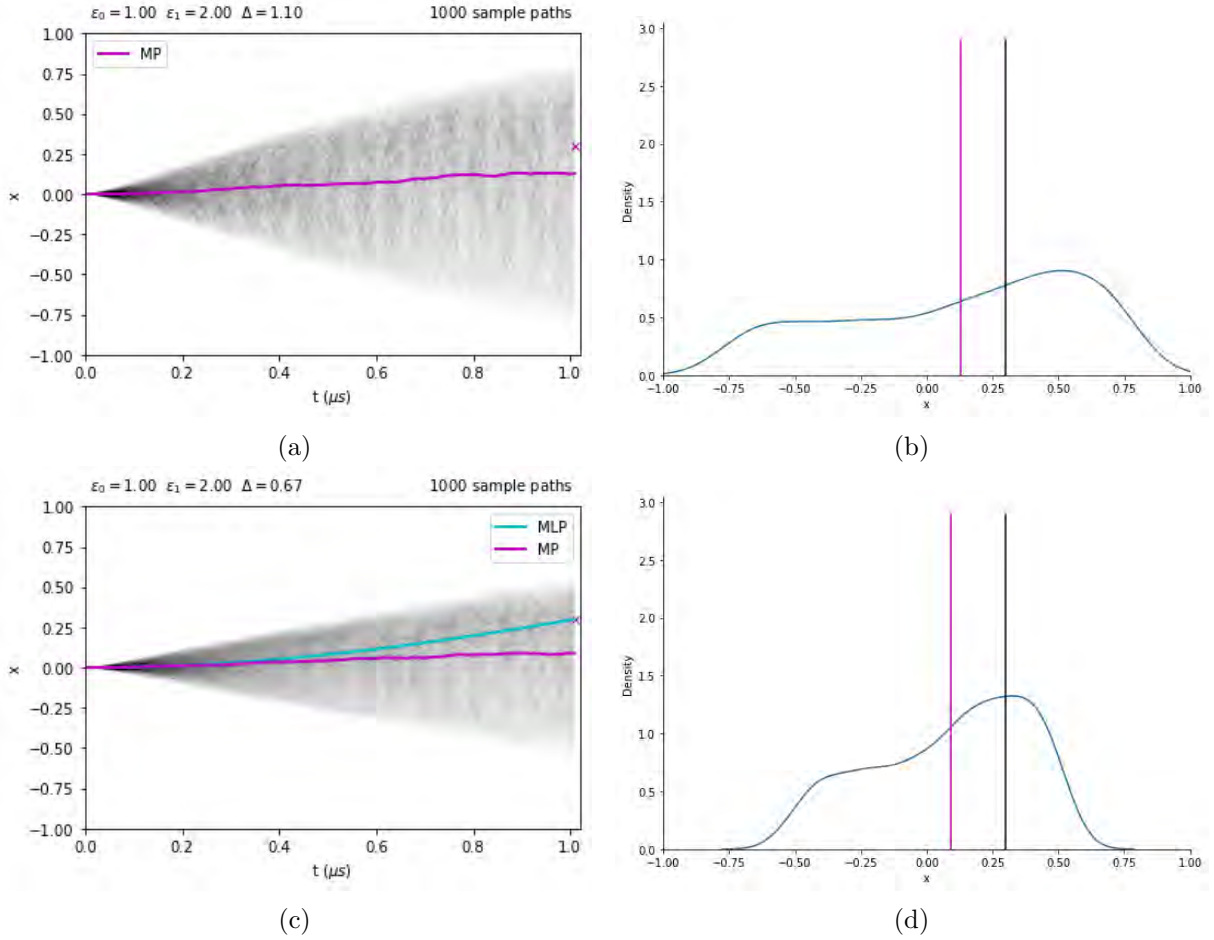


Figure 4.5: The trajectory results (x -component of the qubit) using the optimal Rabi drive from the mean path (numerical search for the minimized trace distance using the Lindblad master equation) and the most likely path (Analytic solution). (a) The quantum trajectories generated with the optimal Rabi drive from the mean path (Gray lines), the target state (Magenta cross), and the mean path (Magenta line). (b) The distribution of the final states of (a), which does not concentrate around the target state (Black line) or the final state of the mean path (Magenta line). (c) The quantum trajectories generated with the optimal Rabi drive from the most likely path (Gray lines), the most likely path (Cyan), the target state (Magenta cross), and the mean path (Magenta line). (d) The distribution of the final state of (c) perfectly concentrated around the target state (Black line). Here, we set the qubit energy $\epsilon_0 = 1.00$, the strength of the dephasing noise is $\epsilon_1 = 2$, the initial state $\mathbf{q}_I = (0, 0, -1)$, the desired target state $\mathbf{q}_F = (0.3, -0.52, -0.8)$, and the total time duration $T = 1$.

It is interesting to note that when the qubit has rotational symmetry around the z -axis, the most likely path and mean path approaches yield completely different optimal Rabi drives. There are more than one the Rabi drive that can provide the maximum fidelity. In Fig. (4.6), a numerical search for the optimal Rabi drive using the mean path

approach yields the optimal Rabi drive to be $\Delta_{\text{op}}^{\text{MP}} = 3.04$, whereas the optimal Rabi drive from the most likely path approach is $\Delta_{\text{op}}^{\text{MLP}} = -1.4$. The average fidelity of the final state from the most likely path approach is $\mathcal{F} \sim 0.974$, while the average fidelity from the mean path approach is $\mathcal{F} \sim 0.975$. The average fidelity of the mean path approach is slightly higher. However, when we look at the actual distribution of the final state in Fig. (4.7), both in the Bloch sphere and spherical coordinates, we find that the mean path control leads to the final states that do not concentrate around the target state as shown in Fig. (4.7 b,d). This means that the higher average fidelity does not mean high success in reaching the target state. As shown in Fig. (4.7 a,c), the most likely path is more suitable to represent the quantum trajectories and also offer better control.

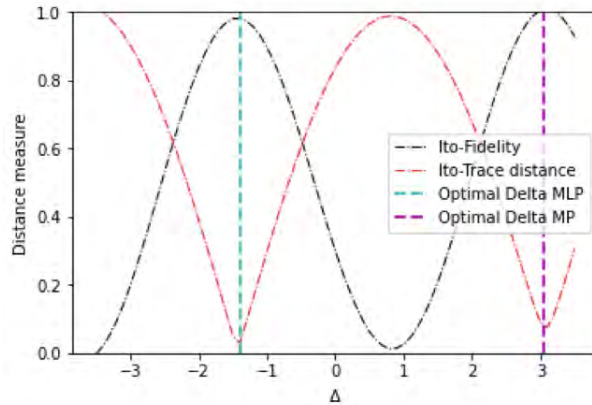


Figure 4.6: An example of the prediction of the optimal Rabi drive from the most likely path, $\Delta_{\text{op}}^{\text{MLP}} = -1.4$ (Cyan line), that does not coincide with the optimal Rabi drive from the mean path. We perform a numerical search by using the Lindblad master equation Eq. (2.7) and maximizes the fidelity (Black line), giving the optimal Rabi drive from the mean path $\Delta_{\text{op}}^{\text{MP}} = 3.04$ (Magenta line). The average fidelity of the most likely path approach is $\mathcal{F} \sim 0.974$, while the average fidelity of the mean path approach is $\mathcal{F} \sim 0.975$. Here, we set the qubit energy $\epsilon_0 = -0.1$, the strength of the dephasing noise $\epsilon_1 = 0.35$, the initial state $\mathbf{q}_I = (0, 0, -1)$, and the desired target state $\mathbf{q}_F = (0.1, 0.9, 0.4)$.

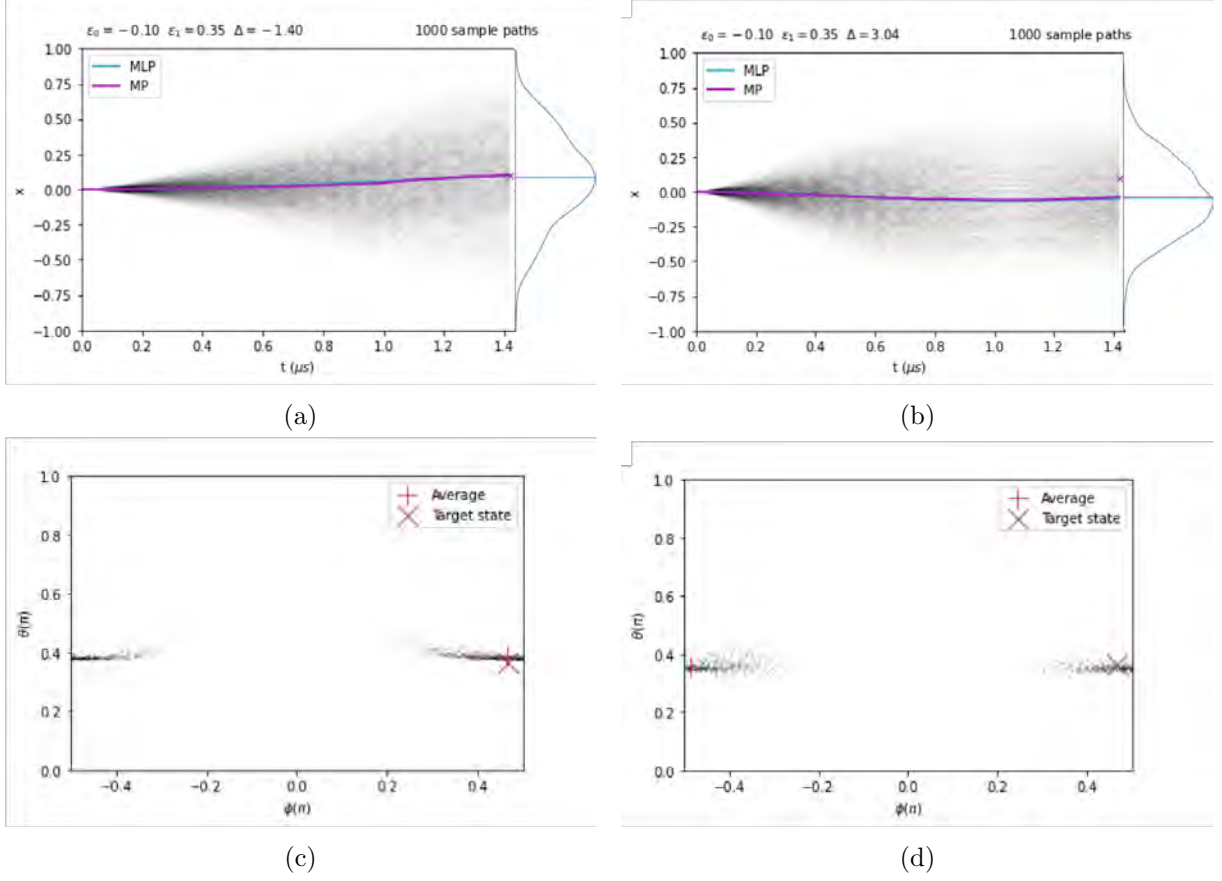


Figure 4.7: The results of distribution of final states in the spherical coordinate, controlled by the optimal Rabi drive from the most likely path and the mean path approaches. The optimal Rabi drive from the most likely path is $\Delta_{\text{op}}^{\text{MLP}} = -1.40$ with the optimal total time duration $T_{\text{op}}^{\text{MLP}} = 1.40$, while the optimal Rabi drive from the mean path is $\Delta_{\text{op}}^{\text{MP}} = 3.04$. (a) and (b) show the quantum trajectories (Gray lines), the most likely path (Magenta line), and the mean path (Cyan line), where the distribution of the final states are attached on the right side of the figure. The optimal Rabi drive from the most likely path is used in (a), while the optimal Rabi drive from the mean path is used in (b). (c) and (d) show the distribution of final states of (a) and (b) in the spherical coordinate respectively. Here, we set the qubit energy $\epsilon_0 = -0.1$, the strength of the dephasing noise $\epsilon_1 = 0.35$, the initial state $\mathbf{q}_I = (0, 0, -1)$, and the desired target state $\mathbf{q}_F = (0.1, 0.9, 0.4)$.

We finally show some results where the most likely path the mean path approaches give similar optimal Rabi drives. In Fig. (4.8), we show that the two approaches are only slightly different. In Fig. (4.8 a), we set $\epsilon_0 > \epsilon_1$ and in Fig. (4.8 b), we consider in the situation of high noise strength $\epsilon_1 > \epsilon_0$. In both cases, the optimal Rabi drive from both approaches lead to averaged high fidelity to the target state.

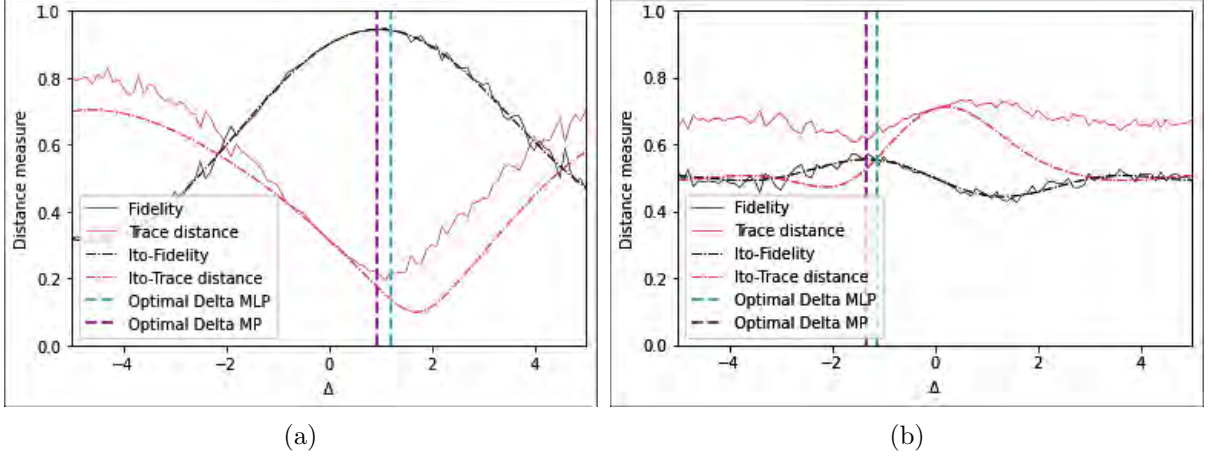


Figure 4.8: The comparison between the most likely path and the mean path approaches in maximizing the average fidelity to the target state. The distance measures are trace distance (Red) and the average fidelity (Black). The smooth line is the average distance measure of final states, and the dot-dashed line is obtained from the mean path. The vertical dashed lines show the optimal Rabi drive from the most likely path (Cyan dot-dashed line) and the mean path (Magenta dot-dashed line). (a) The optimal Rabi drive from the most likely path is $\Delta_{\text{op}}^{\text{MLP}} = 1.20$, whereas the optimal Rabi drive from the mean path is $\Delta_{\text{op}}^{\text{MP}} = 0.94$, setting the qubit energy $\epsilon_0 = 3$, the strength of the dephasing noise $\epsilon_1 = 2$, the initial state $\mathbf{q}_I = (0, 0, -1)$, and the desired target state $\mathbf{q}_F = (0.5, -0.33, -0.8)$. (b) The optimal Rabi drive from the most likely path is $\Delta_{\text{op}}^{\text{MLP}} = -1.11$, whereas the optimal Rabi drive from the mean path is $\Delta_{\text{op}}^{\text{MP}} = -1.32$, setting the qubit energy $\epsilon_0 = -1$, the strength of the dephasing noise $\epsilon_1 = 3$, the initial state $\mathbf{q}_I = (0, 0, -1)$, and the desired target state $\mathbf{q}_F = (0.9, 0.44, 0)$.

Chapter 5

Conclusions

We study the ability to control a quantum state in the presence of environmental noises. In some situations, the standard method for describing the open quantum system is the Lindblad master equation; however, the mean path approach can not always faithfully represent the path of the ensemble of quantum trajectories. The distribution of the final states from the mean path approach may not concentrate around the desired target state, leading us to investigate an alternative means via the most likely path to represent the dynamics of an open quantum system. The other disadvantage of the mean path approach is that to obtain the optimal control by Lindblad master equation (Chapter 2), we can only at best numerically search for optimal control that yields the maximum average fidelity. No analytic methods exist.

We have presented an alternative approach to compute optimal dynamics to control open quantum system via the most likely path, focusing on the qubit state preparation in the presence of dephasing noise problem (In chapter 3). Namely, we study MLP-approach to control the two-level system under noise influenced to evolve the initial state to desired target state with high fidelity. We have modified the stochastic path integral technique for qubit state preparation, given fixed initial and final states. We obtained the most likely path of the quantum trajectories by extremizing the action in stochastic path integral. The advantage of an approach is that we can obtain analytic solutions for qubit state

preparation without Rabi drive ($\Delta = 0$). We have also derived a set of ordinary differential equations that describes the most likely path in qubit state preparation without Rabi drive ($\Delta \neq 0$). In the last of Chapter [3](#), we derived the analytic solution for optimal Rabi drive and time duration control. In particular, we can control the qubit state preparation by using the optimal Rabi drive and time duration, which yields the most likely path to the desired target state. We have also shown the advantage of our approach by comparing the fidelity of optimal Rabi drive and arbitrary control schemes.

In Chapter [4](#), we show the prime example of the optimal Rabi drive from the traditional method, Lindblad master equation, searching for the optimal Rabi drive to control is totally different from the optimal Rabi drive from the most likely path analytical solution. The Rabi drive from the most likely path generates the quantum trajectories that concentrate around the target state and also show the distribution of the final state in the spherical coordinate. The final states from the most likely path approach less spread out than the mean path approach. Moreover, the open quantum system can be extended to more complicated and realistic systems which we hope to explore in the future, such as multiple qubits, inefficient measurement and coloured noise.

Bibliography

- [1] I. Rotter and J. P. Bird. *A review of progress in the physics of open quantum systems: theory and experiment*. Rep. Prog. Phys. 78 114001, 2015.
- [2] V. Semin and F. Petruccione. *Dynamical and thermodynamical approaches to open quantum systems*. Sci Rep 10, 2607, 2020.
- [3] F. Verstraete, M. Wolf, and J. Ignacio Cirac. *Quantum computation and quantum-state engineering driven by dissipation*. Nature Phys 5, 633–636, 2009.
- [4] C. Altafini and F. Ticozzi. *Modeling and Control of Quantum Systems: An Introduction*. IEEE Transactions on Automatic Control, 57(8), 1917.
- [5] S. Glaser, U. Boscain, T. Calarco, and et al. *Training Schrödinger’s cat: quantum optimal control*. Eur. Phys. J. D 69, 279, 2015.
- [6] C. P. Koch. *Controlling open quantum systems: tools, achievements, and limitations*. J. Phys.: Condens. Matter 28 213001, 2016.
- [7] T. Schulte-Herbrüggen, A. Spörl, N. Khaneja, and S. J. Glaser. *Optimal control for generating quantum gates in open dissipative systems*. J. Phys. B: At. Mol. Opt. Phys. 44 154013, 2011.
- [8] A. Chantasri and A. N. Jordan. *Stochastic path-integral formalism for continuous quantum measurement*. Physical Review A 92, 032125, 2015.

- [9] S. Weber, A. Chantasri, J. Dressel, and et al. *Mapping the optimal route between two quantum states*. Nature 511, 570–573 (2014).
- [10] I. L. Chuang D. A. Lidar and K. B. Whaley. *Decoherence-free subspaces for quantum computation*. Phys. Rev. Lett., 1998.
- [11] C. W. Gardiner and P. Zoller. *Quantum Noise*. Berlin, 2000.
- [12] H. M. Wiseman and G. J. Milburn. *Quantum measurement and control*. Cambridge University Press UK, 2010.
- [13] H. P. Breuer and F. Petruccione. *The Theory of Open Quantum Systems*. Oxford University Press, 2002.
- [14] H. Nakazato and S. Pascazio. *Two-Level System with a Noisy Hamiltonian*. Journal of Superconductivity 12, 1999.
- [15] P. Krantz, M. Kjaergaard, F. Yan, T. P. Orlando, S. Gustavsson, and W. D. Oliver. *A quantum engineer’s guide to superconducting qubits*. Applied Physics Reviews 6, 021318, 2019.
- [16] Li et al. *Concepts of quantum non-Markovianity: A hierarchy*, volume 759. Physics Reports, 2018.
- [17] C. W. Gardiner. *Handbook of Stochastic Methods*. Springer, 1985.
- [18] N. G. van Kampen. *Stochastic process in physics and chemistry*. Springer, 2007.
- [19] D. Dong. *Learning Control of Quantum Systems*. Baillieul J. Samad T. (eds) Encyclopedia of Systems and Control. Springer, London, 2020.
- [20] T. Caneva, T. Calarco, and S. Montangero. *Chopped random-basis quantum optimization*. Phys. Rev. A 84, 022326, 2011.

- [21] A. Chantasri, J. Dressel, and A. N. Jordan. *Action Principle for Continuous Quantum Measurement*. Phys. Rev. A 88, 042110, 2013.

Appendix A

Derivation

A.1 Ito Stochastic differential equations to Lindblad master equation

Recall the Hamiltonian

$$\mathcal{H} = (\epsilon_0 + \epsilon_1\eta)\sigma_z/2 - \Delta\sigma_x/2. \quad (\text{A.1})$$

The dynamic of density matrix is

$$\rho_{t+dt} = \mathcal{U}\rho_t\mathcal{U}^\dagger. \quad (\text{A.2})$$

By making use the unitary operator $\mathcal{U} = \exp(-i\mathcal{H}\delta t)$ and the Bloch sphere components $q_i = \text{Tr}(\rho\sigma_i)$

$$\exp(i\theta\hat{v} \cdot \vec{\sigma}) = \cos(\theta)\mathbb{I} + i\sin(\theta)(\hat{v} \cdot \vec{\sigma}). \quad (\text{A.3})$$

Let $\epsilon = \epsilon_0 + \epsilon_1\eta$, $\theta = (-\delta t)(\sqrt{(\Delta^2/4 + \epsilon^2/4)})$, $v_x = \frac{-\Delta/2}{(\sqrt{(\Delta^2/4 + \epsilon^2/4)})}$, and $v_z = \frac{(\epsilon_0 + \epsilon_1\eta)/2}{\sqrt{(\Delta^2/4 + \epsilon^2/4)}}$.

Eq. (A.2) can be rewritten as

$$\begin{aligned} \rho_{t+\delta t} = & \rho_t + i\sin(\theta)\cos(\theta)(v_x[\sigma_x, \rho_t] + v_z[\sigma_z, \rho_t]) \\ & + \sin^2(\theta)\{v_x v_z(\sigma_z \rho_t \sigma_x + \sigma_x \rho_t \sigma_z) + v_x^2 \sigma_x \rho_t \sigma_x + v_z^2 \sigma_z \rho_t \sigma_z - \rho_t\}. \end{aligned} \quad (\text{A.4})$$

In Bloch sphere coordinates,

$$x_{t+\delta t} = x_t + \frac{y_t \epsilon \sin \theta \cos \theta}{\sqrt{(\Delta^2/4 + \epsilon^2/4)}} + \frac{\sin^2 \theta}{\Delta^2/4 + \epsilon^2/4} \left\{ -\frac{z_t \Delta \epsilon}{2} - \frac{x_t \epsilon^2}{2} \right\}, \quad (\text{A.5a})$$

$$y_{t+\delta t} = y_t - \frac{(x_t \epsilon + z_t \Delta) \sin \theta \cos \theta}{\sqrt{(\Delta^2/4 + \epsilon^2/4)}} + \frac{\sin^2 \theta}{\Delta^2/4 + \epsilon^2/4} \left\{ -\frac{y_t \Delta^2}{2} - \frac{y_t \epsilon^2}{2} \right\}, \quad (\text{A.5b})$$

$$z_{t+\delta t} = z_t + \frac{y_t \Delta \sin \theta \cos \theta}{\sqrt{(\Delta^2/4 + \epsilon^2/4)}} + \frac{\sin^2 \theta}{\Delta^2/4 + \epsilon^2/4} \left\{ -\frac{x_t \Delta \epsilon}{2} - \frac{z_t \Delta^2}{2} \right\}. \quad (\text{A.5c})$$

The Lindblad master equation [\(2.7\)](#) is obtained by applying the Ito rule, $\eta^2 \delta t^2 \sim \delta t$, $\delta t^2 = 0$, and averaging over noise realization $\langle \eta \rangle = 0$.

A.2 The analytical solution of the most likely path in state preparation without without Rabi oscillation ($\Delta = 0$)

Firstly, take derivative respect to time Eq. [\(3.11e\)](#).

$$\begin{aligned} \dot{\eta} &= -\epsilon_1 (\dot{p}^x y + \dot{y} p^x - \dot{p}^y x - \dot{x} p^y), \\ \dot{\eta} &= -\epsilon_1 (-\epsilon_0 p^y y - \epsilon_1 \eta p^y y + \epsilon_0 p^x x + \epsilon_1 \eta x p^x - \epsilon_0 p^x x \\ &\quad - \epsilon_1 \eta p^x x + \epsilon_0 y p^y + \epsilon_1 \eta y p^y). \end{aligned} \quad (\text{A.6})$$

Thus, we get

$$\dot{\eta} = 0, \quad (\text{A.7})$$

Then, we can solve the most likely path analytically. For convenient let $\epsilon = \epsilon_0 + \epsilon_1 \eta$.

Solving the ODEs for the trajectory solution

$$\frac{d}{dt} \begin{pmatrix} x \\ y \end{pmatrix} = \begin{pmatrix} 0 & -\epsilon \\ +\epsilon & 0 \end{pmatrix} \begin{pmatrix} x \\ y \end{pmatrix}, \quad (\text{A.8})$$

The trial solution is $(x, y) = (A, B)e^{\lambda t}$

$$\lambda \begin{pmatrix} A \\ B \end{pmatrix} = \begin{pmatrix} 0 & -\epsilon \\ +\epsilon & 0 \end{pmatrix} \begin{pmatrix} A \\ B \end{pmatrix}, \quad (\text{A.9})$$

So the eigenvalue problem is

$$\left[\lambda \begin{pmatrix} 1 & 0 \\ 0 & 1 \end{pmatrix} - \begin{pmatrix} 0 & -\epsilon \\ +\epsilon & 0 \end{pmatrix} \right] \begin{pmatrix} A \\ B \end{pmatrix} = 0, \quad (\text{A.10})$$

$$\begin{vmatrix} \lambda & \epsilon \\ -\epsilon & \lambda \end{vmatrix} = 0, \quad (\text{A.11})$$

$$\lambda = \pm i\epsilon, \quad (\text{A.12})$$

When $\lambda = i\epsilon$,

$$\begin{pmatrix} i\epsilon & \epsilon \\ -\epsilon & i\epsilon \end{pmatrix} \begin{pmatrix} A \\ B \end{pmatrix} = 0, \quad (\text{A.13})$$

$$\begin{pmatrix} A \\ B \end{pmatrix} = c_1 \begin{pmatrix} -1 \\ i \end{pmatrix}, \quad (\text{A.14})$$

When $\lambda = -i\epsilon$,

$$\begin{pmatrix} -i\epsilon & \epsilon \\ -\epsilon & -i\epsilon \end{pmatrix} \begin{pmatrix} A \\ B \end{pmatrix} = 0, \quad (\text{A.15})$$

$$\begin{pmatrix} A \\ B \end{pmatrix} = c_2 \begin{pmatrix} i \\ -1 \end{pmatrix}, \quad (\text{A.16})$$

The general solution is

$$\begin{pmatrix} x \\ y \end{pmatrix} = c_1 \begin{pmatrix} -1 \\ i \end{pmatrix} e^{i\epsilon t} + c_2 \begin{pmatrix} 1 \\ i \end{pmatrix} e^{-i\epsilon t}. \quad (\text{A.17})$$

By introducing $c_3 = i(c_1 + c_2)$, and $c_4 = c_1 - c_2$, we obtain the general solution

$$\begin{pmatrix} x \\ y \end{pmatrix} = c_3 \begin{pmatrix} -\sin(\epsilon t) \\ \cos(\epsilon t) \end{pmatrix} + c_4 \begin{pmatrix} -\cos(\epsilon t) \\ -\sin(\epsilon t) \end{pmatrix}. \quad (\text{A.18})$$

A.3 Rabi drive and total time duration control

Consider derivative of Eq. (3.20h) and let $\epsilon \equiv \epsilon_0 + \epsilon_1 \eta$.

$$\dot{p}^y z + \dot{z} p^y = \dot{p}^z y + \dot{y} p^z, \quad (\text{A.19a})$$

$$(\epsilon p^x + \Delta p^z) z + -\Delta y p^y = -\Delta p^y y + (\epsilon x + \Delta z) p^z, \quad (\text{A.19b})$$

$$p^x z = p^z x. \quad (\text{A.19c})$$

Again, consider derivative of Eq. (A.19c)

$$\dot{p}^x z + \dot{z} p^x = \dot{p}^z x + \dot{x} p^z, \quad (\text{A.20a})$$

$$(-\epsilon p^y) z + -\Delta y p^x = -\Delta p^y x + (-\epsilon y) p^z, \quad (\text{A.20b})$$

$$p^x y = p^y x. \quad (\text{A.20c})$$

Substitute Eq. (A.20c) into Eq. (3.20g) we obtain

$$\eta = 0. \quad (\text{A.21})$$

Lead to

$$\dot{x} = -\epsilon_0 y, \quad (\text{A.22a})$$

$$\dot{y} = +\epsilon_0 x + \Delta z, \quad (\text{A.22b})$$

$$\dot{z} = -\Delta y. \quad (\text{A.22c})$$

We obtain the general solution

$$x = c_4 \frac{\epsilon_0}{\Delta} \cos(\omega t) + c_5 \frac{\epsilon_0}{\Delta} \sin(\omega t) - c_1 \frac{\Delta}{\epsilon_0}, \quad (\text{A.23a})$$

$$y = -c_5 \frac{\omega}{\Delta} \cos(\omega t) + c_4 \frac{\omega}{\Delta} \sin(\omega t), \quad (\text{A.23b})$$

$$z = c_4 \cos(\omega t) + c_5 \sin(\omega t) + c_1, \quad (\text{A.23c})$$

$$\omega = \sqrt{\Delta^2 + \epsilon_0^2}, \quad (\text{A.23d})$$

where $c_1 = (\epsilon_0^2 z_I - \epsilon_0 \Delta x_I)/\omega^2$, $c_4 = (\Delta^2 z_I + \epsilon_0 \Delta x_I)/\omega^2$, $c_5 = -y_I(\Delta)/\omega$. Apply the initial condition $(x_I, y_I, z_I) = (0, 0, -1)$, we obtain

$$x = \frac{-\epsilon_0 \Delta}{\omega^2} \cos(\omega t) + \frac{\epsilon_0 \Delta}{\omega^2}, \quad (\text{A.24a})$$

$$y = -\frac{\Delta}{\omega} \sin(\omega t), \quad (\text{A.24b})$$

$$z = -\frac{\Delta^2}{\omega^2} \cos(\omega t) - \frac{\epsilon_0^2}{\omega^2}, \quad (\text{A.24c})$$

$$\omega = \sqrt{\Delta^2 + \epsilon_0^2}. \quad (\text{A.24d})$$

Let consider in the final time of controlled state (x_F, y_F, z_F) . Let multiply x_F by Δ and multiply z_F by ϵ_0 . We then obtain the Rabi drive,

$$\Delta = \epsilon_0 \frac{z_F + 1}{x_F}. \quad (\text{A.25})$$

And we obtain the total time duration from x_F ,

$$T = \frac{1}{\omega} \arccos\left(1 - \frac{x_F \omega^2}{\epsilon_0 \Delta}\right). \quad (\text{A.26})$$

Assume that we can choose the sign of ϵ_0 . From the arccos is a periodic function then we can select the shortest time by changing the sign of ϵ_0 . Sign of ϵ_0 depend on the octant in three dimensions. If we desire the final state in octant $(+, -, \pm)$ and $(-, +, \pm)$. Then, we use the positive sign of ϵ_0 . In contrast, the final state in octant $(+, +, \pm)$ and $(-, -, \pm)$.

Then, we use the minus sign of ϵ_0 . Lead to

$$\epsilon_0 \rightarrow -\frac{x_F y_F}{|x_F y_F|} \epsilon_0, \quad (\text{A.27a})$$

$$\epsilon_0 = -\text{sgn}[x_F y_F]. \quad (\text{A.27b})$$

We should also mention that the Rabi drive and total time duration, in general, will write in any initial conditions,

$$\Delta = \text{sgn}[x_F y_F] \frac{z_I - z_F}{x_F - x_I}, \quad (\text{A.28a})$$

$$T = \frac{1}{\omega} \arccos\left(\frac{\Delta \omega x_F c_4 - \Delta \epsilon_0 y_F c_5 + c_1 c_4 \Delta^2 \omega / \epsilon_0}{\epsilon_0 \omega (c_4^2 + c_5^2)}\right). \quad (\text{A.28b})$$

Appendix B

Distance measure

Distance measures must be considered when comparing the similarities of the post-selected and controlled states. The trace distance and fidelity are measurements of how close two quantum states are to each other. The trace distance for a qubit is half of the Euclidean distance, $0 \leq D \leq 1$ which mean the best possible is $D = 0$ when the final and target state are the same position on Bloch sphere. The fidelity is the projection of the final state onto the target state, $0 \leq F \leq 1$ which mean the best possible is $F = 1$ when the final and target state are the same state in Hilbert space. We can write them in the form of Bloch sphere coordinates, the target state $\mathbf{r} = (x_1, y_1, z_1)$ and the controlled state $\mathbf{s} = (x_2, y_2, z_2)$.

B.1 Trace distance

The trace distance between the quantum states ρ and σ is given by

$$D(\rho, \sigma) = \frac{1}{2} \text{Tr}|\rho - \sigma|, \quad (\text{B.1})$$

For Geometric view (Bloch's sphere) Let $\rho = \frac{\mathbb{I} + \mathbf{r} \cdot \boldsymbol{\sigma}}{2}$ and $\sigma = \frac{\mathbb{I} + \mathbf{s} \cdot \boldsymbol{\sigma}}{2}$. We obtain

$$D(\rho, \sigma) = \frac{1}{2} \text{Tr}|\rho - \sigma| = \frac{1}{4} \text{Tr}|(\mathbf{r} - \mathbf{s}) \cdot \boldsymbol{\sigma}|. \quad (\text{B.2})$$

The matrix $|(\mathbf{r} - \mathbf{s}) \cdot \sigma|$ has eigenvalues $\pm|(\mathbf{r} - \mathbf{s})|$ so that

$$D(\rho, \sigma) = \frac{1}{2}|\mathbf{r} - \mathbf{s}|. \quad (\text{B.3})$$

Note that the distance between points in Euclidean space, \mathbb{R}^n , is $d(\mathbf{r}, \mathbf{s}) = \sqrt{\sum_{i=1}^n |r_i - s_i|^2} = |\mathbf{r} - \mathbf{s}|$. Thus, the trace distance for qubits is half of the Euclidean distance in \mathbb{R}^3 .

$$D(\rho, \sigma) = \frac{1}{2}\sqrt{(x_1 - x_2)^2 + (y_1 - y_2)^2 + (z_1 - z_2)^2}. \quad (\text{B.4})$$

B.2 Fidelity

The fidelity of state ρ and σ is defined as

$$F(\rho, \sigma) = [\text{Tr}(\sqrt{\rho^{1/2}\sigma\rho^{1/2}})]^2. \quad (\text{B.5})$$

It is possible to obtain simpler formulae for F . These were given by Hubner. Consider M be Hermitian matrix with positive eigenvalues λ_1, λ_2 .

$$\text{Tr}(\sqrt{M}) = \sqrt{\lambda_1} + \sqrt{\lambda_2}. \quad (\text{B.6})$$

$$(\text{Tr}(\sqrt{M}))^2 = \lambda_1 + \lambda_2 + 2\sqrt{\lambda_1}\sqrt{\lambda_2} = \text{Tr}(M) + 2\sqrt{\det M}. \quad (\text{B.7})$$

Taking,

$$M = \rho^{1/2}\sigma\rho^{1/2}. \quad (\text{B.8})$$

We get,

$$\text{Tr}(M) = \text{Tr}(\rho\sigma), \quad \det M = \det \rho \det \sigma. \quad (\text{B.9})$$

Then,

$$F(\rho, \sigma) = \text{Tr}(\rho\sigma) + 2\det \rho \det \sigma. \quad (\text{B.10})$$

We get the following result, if at least one of them is pure state (the determinant of pure state is zero),

$$F(\rho, \sigma) = \text{Tr}(\rho\sigma). \quad (\text{B.11})$$

For Geometric view (Bloch sphere). Let $\rho = \frac{\mathbb{I}+r\cdot\boldsymbol{\sigma}}{2}$ and $\sigma = \frac{\mathbb{I}+s\cdot\boldsymbol{\sigma}}{2}$. We obtain,

$$F(\rho, \sigma) = \frac{1}{2}(1 + x_1x_2 + y_1y_2 + z_1z_2). \quad (\text{B.12})$$